

## Influence of anodizing process on tensile strength AA 6061 T6

Putu Hadi Setyarini<sup>1\*</sup>, Slamet Wahyudi<sup>1</sup>, Purnomo<sup>2</sup>, Dwi Hadi Sulistyarini<sup>3</sup>, Avissena Izhar Mafazi<sup>1</sup>,  
Made Sandya Devandhika<sup>1</sup>

<sup>1</sup> Mechanical Engineering Department, Faculty of Engineering, Brawijaya University, Malang 65145, Indonesia

<sup>2</sup> Mechanical Engineering Department, Faculty of Engineering, Universitas Muhammadiyah Semarang, Semarang 50723, Indonesia

<sup>3</sup> Industrial Engineering Department, Faculty of Engineering, Brawijaya University, Malang 65145, Indonesia

\* Corresponding author: [putu\\_hadi@ub.ac.id](mailto:putu_hadi@ub.ac.id)

### ABSTRACT

To determine the effect of sulfuric acid electrolyte concentration and the most optimal electrical potential during the anodizing process on the tensile strength of aluminum alloy 6061 T6. The anodizing process of aluminum alloy is carried out at different electrolyte concentrations, which are 10, 20 and 30% of the volume of sulfuric acid used. As a cathode, carbon rods are used. The duration of the process for each electrolyte concentration is 15 minutes, while the potential used is 10 V, 20 V and 30 V. The tensile testing process is carried out using a Universal Testing Machine and surface morphology is investigated using Scanning Electron Microscopy Phenom G2. Anodizing process using 20% sulfuric acid electrolyte concentration and 20 V potential has the highest ultimate tensile strength. However, on the surface morphology, the pore size starts to enlarge when compared to the potential and concentration of the electrolyte below. As for the potential and higher concentrations of sulfuric acid, there is a decrease in tensile strength and an increase in pore size. This can make an understanding concept of how AA 6061 T6 reacts to the tensile stress after anodizing process is carried out, so that it can later be applied to industry and machinery.

**Key words:** Tensile strength, Electrolyte, Sulfuric acid

### 1. INTRODUCTION

Aluminum is a lightweight metal that is quite prominent and is widely used in everyday life. This material is used in a wide range of fields, not only for household appliances but also in the industrial world, building construction materials and many other uses as has been reviewed by [1], [2] and [3]. This development is based on its properties which are lightweight, corrosion resistant, easily manufactured and quite economical as previously reported by [4], [5] and [6].

This material is quite unique because it is able to form a barrier oxide layer that is firmly bound to its surface, and if the layer is damaged, it will be formed again naturally. On aluminum surfaces that are abraded and exposed to air, the thickness of the barrier oxide layer is only about 1 nm, however, the coating is still very effective at protecting aluminum from corrosion.

One way to improve and perfect the surface quality of aluminum is the anodizing process. With this anodizing process, aluminum will be obtained which has better properties. Increased wear resistance, increased heat resistance, increased hardness and increased corrosion resistance [7]-[10]. Besides improving the material properties of a product, this anodizing process also beautifies the appearance of a product.

Ito et al. [11], Capraz et al. [12] and Lee et al. [13] state that the aluminum anodizing process is an electrochemical method to convert aluminum into aluminum oxide ( $Al_2O_3$ ) on the surface to be coated to produce a thicker oxide layer than the naturally formed oxide layer so as to improve the physical and mechanical properties of metals. This can be achieved by making the workpiece as an anode which is then dipped in the appropriate electrolyte cell. Not all metals can be anodized due to differences in physical and mechanical properties. While some other metals can be anodized, including aluminum, titanium and magnesium, but only aluminum is widely used in the anodizing industry [14-17]. The main thing that can later be obtained through this process is the improvement of both the oxide layer in terms of nanobowls [18], nanowells [19], inverted nanocones [20], [21] and nanospikes [22]-[24]. One of the advantages of this process is the aluminum oxide layer ( $Al_2O_3$ ) produced from the anodizing process is different from the naturally formed oxide layer because anodizing can produce an oxide layer with a thickness that can reach 500 times and hardness up to 2 times

that of aluminum without anodizing. Other researchers various characteristics for metals and non metals [25]-[27].

In this aluminum anodizing experiment using graphite rods as cathodes, with sulfuric acid electrolyte solution. By changing the concentration of sulfuric acid electrolyte and the potential given during the anodizing process, we can find out the effect of these variables in forming the oxide layer on the surface of the substrate. In this experiment the potential used is 10 V, 20 V and 30 V, with sulfuric acid concentrations of 10%, 20% and 30% (% Wt) and the time used for the anodizing process is 15 minutes.

**2. EXPERIMENTAL METHOD**

**2.1. Material**

The material used in this study was aluminum alloy 6061 T6 with the composition as listed in Table 1. The material was then formed according to the tensile test specimen. In this study, the specimens were anodized using a current of 1 A, sulfuric acid electrolytes with concentrations of 10%, 20% and 30% with anodizing time of 15 minutes.

**Table 1 :** Composition of AA 6061 T6

Element	Composition (%Wt)
Si	0.80
Fe	0.60
Cu	0.18
Mn	0.06
Mg	0.93
Cr	0.06
Zn	0.10
Ti	0.07
Al	Balance

*Anodizing process*

Before the anodizing process is carried out, the test material is first cleaned and mached using rubbing paper with a roughness level, respectively 100, 500, 1000 and 2000 using a centrifugal sandpaper machine to obtain a smooth aluminum surface. After that proceed with the cleaning process which aims to clean the anodized part in order to obtain a satisfactory final result. The cleaning liquid has a composition in the form of sodium carbonate (Na<sub>2</sub>CO<sub>3</sub>) with a solution concentration of 5gr / liter. After finishing the cleaning process, the aluminum surface part must not be touched by hand because it can cause dirt and grease back to stick to the surface of the material. The next process is the etching process which aims to remove the natural oxide layer that is on the surface of aluminum which cannot be removed by the previous process be it cleaning or rinsing. In addition,

the etching process is also intended to make the surface of the workpiece smoother. The composition of the etching liquid in the form of a solution of caustic soda (NaOH) with a concentration of 100 gr / liter. The last is the desmut process. This process has the aim to clean up the black patches caused by the etching process. The commonly used solution is a mixture of phosphoric acid (H<sub>3</sub>PO<sub>4</sub>) with a ratio of 75% plus 15% sulfuric acid (H<sub>2</sub>SO<sub>4</sub>), and 10% nitric acid (HNO<sub>3</sub>).

While the next process is the anodizing process. This process is an electrochemical coating process that is carried out to form an oxide layer on the surface of aluminum. The aluminum that will be anodized is dipped in an electrolyte solution in the form of sulfuric acid (H<sub>2</sub>SO<sub>4</sub>) with concentrations of 10%, 20% and 30%, respectively. Then the electrical potential of 10V, 20V and 30V is applied to the electrolyte solution. Aluminum is connected by positive current (+) which acts as an anode. Whereas what acts as a cathode is graphite rods. The distance between the anode and cathode is 5 cm with the temperature of the solution ranging from 25 ± 20C and the processing time is 15 minutes. The current passing through the aluminum part to be anodized causes the surface of the aluminum (anode) to oxidize and form aluminum oxide. The formed oxide layer is shaped like a honeycomb structure (honeycomb) which has many microscopic pores.

**2.2. Tensile Testing and Surface Morphology**

Test specimens will be formed according to the standards and specifications of ASTM B 557-02. The shape of the specimen is important because we must avoid the occurrence of fractures or cracks in the grip area or the other. So standardization of the shape of the test specimen is intended so that cracks and fractures occur in the gage length area. The material to be made of the test specimen is aluminum sheet-shaped with a thickness of 1 mm. Then from the sheet shape the specimen is cut into a ready to pull test form. Dimensions of tensile strength specimens can be seen in Figure 1 and Table 2.

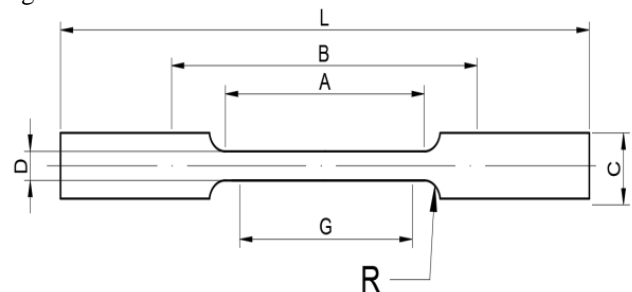


**Figure 1:** Tensile Strength Testing Specimen

**Table 2:** Dimensions of Tensile Test Specimens

Measurement	Size (mm)
G - Potential Concentration Length of Specimen	50.8
D - Diameter	6.35
R - Fillet	76.2

A - Length of specimen reduction	557.15
L - Total Length of Specimen	228.6
B - Length between grips	114.3
C - Final Diameter of Specimen	9.525

Tensile strength testing is carried out using a Universal Testing Machine with a specimen withdrawal speed of 15mm/s. Observation of aluminum surface morphology after anodizing process was carried out using scanning electron microscopy (SEM) Phenom G2 with a magnification of 4000X.

### 3. RESULTS AND DISCUSSION

Tensile testing is a test that aims to get the information of the properties and state of a metal. The length increase that occurs due to the addition of the load is no longer directly proportional, the same increase in load will result in an increase in the length that is greater and one time there is an increase in length without any additional load, the test rod grows longer by itself. This test obtained a tensile load relation curve (F), towards the specimen extension ( $\Delta L$ ). These curves will then be converted into engineering potential curves and engineering spaces and used to obtain the mechanical properties of the metal being tested.

Stress - strain curve diagrams are needed in tensile testing, because to analyze a material that is tensile tested. Tensile test data obtained will be compared between specimens without treatment and treatment specimens to determine changes in strength. Data to be compared are yield strength, UTS (ultimate tensile strength) and elongation values.

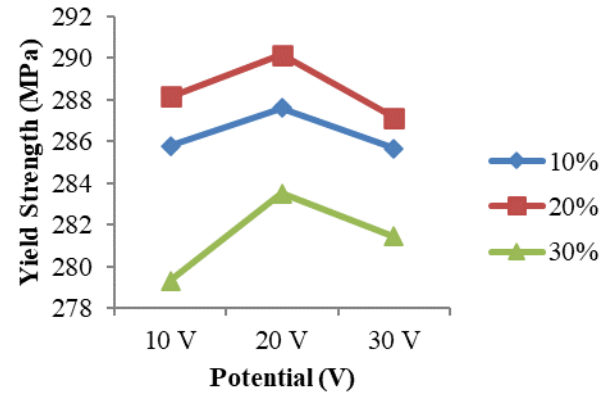
From tensile testing for AA 6061 T6 specimens that did not undergo anodizing process, the yield strength was 246,966 MPa, ultimate tensile strength was 314,481 MPa and elongation was 23,625%.

Figure 2 shows the relationship between yield strength and the percentage of sulfuric acid used in the anodizing process. It appears that a sulfuric acid mixture of 20% in an electrolyte solution has a higher yield potential compared to a mixture of sulfuric acid 10% and 30% in all potential measurements used. After undergoing the anodizing process, it appears that this process is able to increase the tensile strength of AA 6061 T6.

From the test results it is known that the highest yield point is obtained from aluminum which undergoes anodizing process at a potential 20 V by using sulfuric acid electrolytes with a concentration of 20% of 290,168 N/cm<sup>2</sup>. While the lowest value was obtained in the anodizing process carried out with an electrolyte solution with a concentration of H<sub>2</sub>SO<sub>4</sub> of 30% with a yield strength of 281,453 N/cm<sup>2</sup>. It can be said that yield strength is the strength needed to produce the specified small amount of plastic deformation. The yield strength is the

starting point of a material material or metal begins to be plastic deformed.

This mechanical property shows the strength of the material against plastic deformation. The results obtained from this test are used to determine the minimum load required for a material or metal to be deformed plastic.



**Figure 2:** Relationship of Potential and Yield Strength at different concentrations of sulfuric acid after anodizing process

The same thing also appears in Figure 3 where the relationship between potential used and the ultimate tensile strength is illustrated in the variation in the amount of sulfuric acid used in electrolyte solutions. Variation of 20% sulfuric acid has the highest ultimate tensile strength value, especially at a potential of 20 V. The lowest ultimate tensile strength value of 311,573 N / cm<sup>2</sup> is obtained in the anodizing process using a sulfuric acid electrolyte solution with 30% concentration with potential during the 30V process. The highest ultimate tensile strength value was obtained for 30 V potential with a concentration of H<sub>2</sub>SO<sub>4</sub> solution of 30% valued at 311, 573 N / cm<sup>2</sup>.

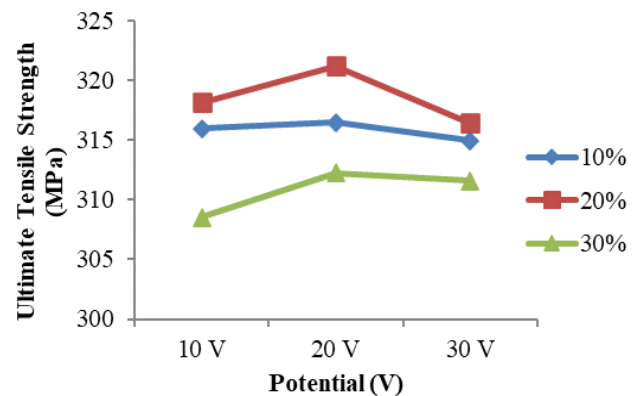


**Figure 3:** The relationship between ultimate tensile strength for anodizing results with different concentrations of electrolyte solutions

The tensile strength of the metal material will show the ability of the material to withstand the tensile forces before undergoing cross section changes or shrinkage. In this

condition, the tensile force works at maximum conditions. So that the working potential is the maximum potential. Maximum stress is the maximum load or force that can be held by material or metal before undergoing cross section or shrinkage changes. This value illustrates the tensile strength of the material.

Meanwhile Figure 4 shows the potential relationship used during the anodizing process with the increase in length during the tensile testing process. It appears that the addition of viscosity of sulfuric acid electrolyte solution can increase the tenacity of AA 6061 T6 after anodized. However, the potential 20 V still has the highest elongation when compared to other potentials.

Ductility of metal is a property that shows the ability of metal materials to increase in length when under load or tensile strength. This quantity is usually referred to as elongation. The tensile stress curve of the tensile test results can be seen in the image below. Strain is denoted by  $\epsilon_f$ . The  $\epsilon_f$  notation is the total strain of material or metal until breaking occurs. Total stretch or elongation is a combination of uniform elongation and elongation that occurs after the material has contracted until it breaks. This strain value indicates the ductility of the material and is usually expressed as an extension percentage. This data shows the amount of length increase that can be given by the material until the break.

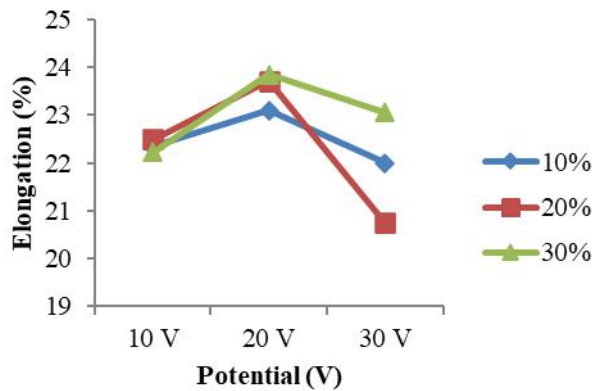


**Figure 4:** Potential relationship in the anodizing process with the increase in material length after tensile testing

Meanwhile from surface observation using scanning electron microscopy with a magnification of 100  $\mu\text{m}$  in Figure 5 shows the surface morphology after the anodizing process has been completed at a potential 20 V. It appears in Figure 5a, where the anodizing process with a concentration of sulfuric acid of 10%, the surface begins to appear several pores that are spread evenly on the surface of aluminum. A much larger pore is seen on the surface of aluminum after anodizing with a much higher concentration of sulfuric acid as shown in Figure 5b with the concentration of sulfuric acid used in the anodizing process of 20%. While for anodized aluminum with a concentration of  $\text{H}_2\text{SO}_4$  of 30% as shown in Figure 5c

shows the pore formed is getting bigger with an uneven size. The pores are spread evenly on the surface of aluminum.

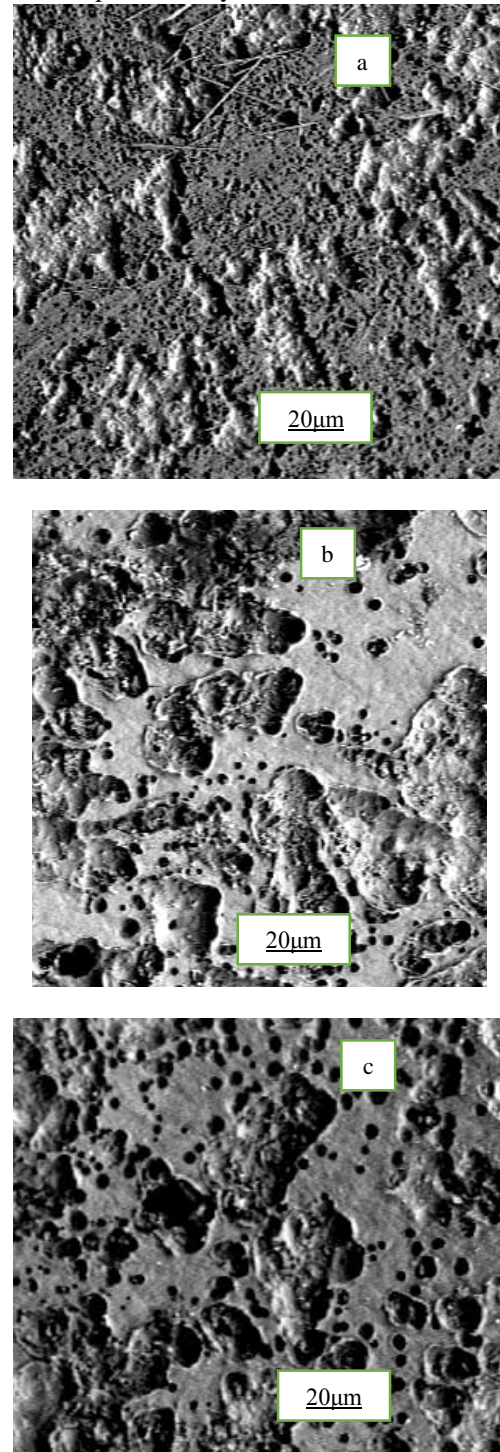


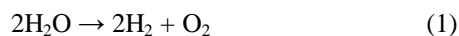
**Figure 5:** Surface morphology of AA 6061 T6 after anodizing at 20 V potential and different concentrations of sulfuric acid (a) 10% (b) 20% (c) 30%

It can be concluded that the overall surface morphology shows the same characteristics as the pores on the surface of the anodized layer which have an unequal size and uneven distribution on the anodized AA 6061 T6 surface, because an increase in potential will increase the volume of expansion during the pore formation process metal face / oxide. This

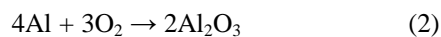
volume of expansion will make the oxide move along the oxide wall. The higher the potential the current density will also increase which will also increase the volume of expansion, so that more oxides move upwards. The pore formation process as detected in the anodized aluminum surface morphology with different concentrations of sulfuric acid in Figure 5(a),(b),(c) shows that the formation of the oxide layer has an unequal velocity. The grain size formed after the anodizing process appears to begin to show a more homogeneous size as the potential increases. The rate of formation of the oxide layer affects the process of atom diffusion and nucleation during the growth of the oxide layer.

At a low potential formation rate, the ability of aluminum atoms to move towards the substrate is so low that the process of forming the oxide layer on the surface of the substrate also takes longer than the anodizing process with a higher potential. This will result in a layer that is formed almost no difference from the substrate because the current density that occurs during the nucleation process is quite low, so that later will form a grain that has a large size.

When a given potential increases, the speed of the process of forming the oxide layer will also be faster because the number of aluminum atoms moving on the surface of the substrate also increases. This will result in a faster nucleation process so that the grains formed will be more homogeneous in size. The anodized oxide layer has a different structure to the naturally formed oxide layer, where the layer has a porous hexagonal pillar structure that has unique characteristics that enhance the mechanical properties of the aluminum surface. This can be explained as follows. When the component to be anodized is dipped into a sulfuric acid electrolyte with a DC current, the following reaction will occur:



Oxygen produced outside the anodized component reacts with the reactive aluminum surface to form aluminum oxide:



At the beginning when the current is flowed into the electrolyte, a thin non-porous dielectric undercoating will form, known as the barrier layer. This layer will grow proportionally to the given potential until it reaches a thickness of about 0.02  $\mu\text{m}$ . This layer has very extreme electrical resistance. At the anodizing potential of 12-20 volts, with a constant potential the current density theoretically drops rapidly, and the growth of the layer stops. With heating due to electrical energy and the ability of electrolytes used to absorb the layer, it will attack the weakest point of the crystal lattice and the pores will be created to form the honeycomb structure of aluminum oxide. The formation

of an oxide layer on the anodized metal surface depends on the type of solution used as an electrolyte, the oxide base layer (barrier type oxide film) and the porous oxide film (porous oxide film) can form during the anodization process. The resulting oxide layer has a porous or porous structure with a hexagonal structure, with a pore in the middle.

On the surface of the oxide layer that is formed in the anodizing process, there are millions of cells per  $\text{cm}^2$ , whose size is a function of the potential process. Pore size is influenced by many factors such as the type of electrolyte, temperature and the relationship between potential and current used. The structure of the oxide layer formed at anodizing using phosphoric acid, sulfuric acid, chromic acid and oxalic acid as the electrolyte, only differ in pore size and cells. In general, the oxide layer resulting from the anodizing process has the following characteristics: One, hard, alumina ( $\text{Al}_2\text{O}_3$ ) has a hardness comparable to sapphire. This layer is also insulative, transparent and resistant to load. There are no flakes on the surface. The oxide layer formed from this process will increase abrasive resistance, the ability of metal electrical insulators, and the ability to absorb dyestuffs to produce variations in the appearance of colors on the anodized surface. Aluminum and its alloys are resistant to atmospheric corrosion due to the protective oxide layer which is quickly formed when aluminum metal is exposed to air.

The formation of an oxide layer on the anodized metal surface depends on the type of solution used as an electrolyte, the oxide base layer (barrier type oxide film) and the porous oxide film (porous oxide film) can form during the anodizing process. The resulting oxide layer has a porous or porous structure with a hexagonal structure, with a pore in the middle. The base layer is a thin and dense layer, which functions as a layer between the pore layer and the base metal.

The porous structure that arises in the oxide layer is the result of equilibrium between the formation reactions of the oxide layer dissolving. Initially the pore layer formed by the elongated cylinder but because it later contacted the other oxides on the sides, the oxide layer transformed into an elongated hexagonal channel. The process of forming an oxide layer can be examined by observing and observing changes in current at a fixed anodizing potential or changes in potential at fixed currents. The process of forming the oxide layer can be divided into four main stages, namely the addition of a barrier layer which is characterized by a decrease in current flowing.

This barrier layer is an aluminum oxide layer that is thickened due to an oxidation reaction on the metal surface. As a result of thickening, the obstacles caused become greater. That is what causes a decrease in current during the formation of the barrier layer. After the barrier layer thickens, pore seeds begin to appear near the boundary between the

oxide and solution. At this stage the current in the rectifier decreases and will reach the minimum point when this stage stops. Then a pore initiation is formed which forms the formation of a porous oxide structure.

The pore shape at this stage is imperfect and an increase in current flows. The current that flows will continue to increase with the more perfect morphology of the oxide layer. This increase occurs until at some point the current that flows will be constant when the porous structure has formed perfectly. The thickness of the film layer from the anodizing process will increase with the time used. However, the rate of increase of the thickness of the oxide layer due to the anodizing process also depends on several factors such as concentration, temperature, potential and current density and the type of metal alloy.

#### 4. CONCLUSION

the AA 6061 T6 anodizing process using an electric potential of 20 V and sulfuric acid electrolytes of 20% Wt have the highest UTS and increase in specimen length when compared to specimens anodized by using different electrical potentials and other electrolyte concentrations.

Pores formed under these conditions begin to have a much larger size compared to aluminum which is anodized at lower concentrations of electrolyte solution, but smaller than AA 6061 T6 which undergoes anodizing processes in sulfuric acid solutions with higher concentrations. This can occur because of increased concentration in relation to the characteristics of the coating, metal loss that occurs in the anodizing process.

Increasing the excess concentration will result in the dissolution of the film layer, so it is necessary to have the right composition of the electrolyte solution to get the optimal film layer. Besides the potential effects on the anodizing process, where it can be seen that the higher the potential used in the anodizing process, the greater the distance between the pores, but the higher the potential used in the anodizing process, the pore density will decrease

#### ACKNOWLEDGEMENT

The research work is supported by PNPB 2019, Faculty of Engineering, Brawijaya University, Indonesia

#### REFERENCES

1. G. E. J. Poinern, N. Ali, D. Fawcett, (2011). **Progress in Nano-Engineered Anodik Aluminum Oxide Membrane Development**, *Materials*, 4, 487-526  
doi:https://doi.org/10.3390/ma4030487
2. P. H. Setyarini, R. Soenoko, A. Suprpto, Y. S. Irawan, (2016). **Properties of Electrochemical Impedance and Surface Characteristics of Anodized AA 6061**. *International Review Mechanical Engineering*, 10, 140-144  
doi:https://doi.org/10.15866/ireme.v10i3.8751
3. G. E. Thompson, (1997). **Porous Anodik Alumina: Fabrication, Characterisation And Application**. *Thin Solid Films*, 297, 192-201  
doi :https://doi.org/10.1016/S0040-6090(96)09440-0
4. A. Vagaska, E. Fechova, P. Michal, M. Gombar, (2016). **The Influence of Input Factor of Aluminum Anodizing Process on Resulting Thickness and Quality of Aluminum Oxide Layer**. *Procedia Engineering*, 149, 512-519  
doi:https://doi.org/10.1016/j.proeng.2016.06.699
5. O. Jessensky, F. Muller, U. Gosele, (1998). **Self Organized Formation of Hexagonal Pore Arrays in Anodic Alumina**. *Applied Physics. Letters*, 72, 1173-1175  
doi :https://doi.org/10.1063/1.121004@apl.2019.APLC LASS2019.issue-1
6. Y. Lin, Q. Lin, X. Liu, Y. Gao, J. He, W. Wang, Z. Fan, (2015). **A Highly Controllable Electrochemical Anodization Process to Fabricate Porous Anodic Aluminum Oxide Membranes**, *Nanoscale Research Letters*, 10, 495.
7. J. Hirsch, T. Al-Samman, (2013). **Superior Light Metals by Texture Engineering : Optimized Aluminum and Magnesium Alloys for Automotive Engineering**, *Acta Materialia*, 61, 818-843  
doi:https://doi.org/10.1016/j.actamat.2012.10.044
8. M. Bononi, M. Conte, R. Giovanardi, A. Bozza, (2017). **Hard anodizing of AA2099-T8 Aluminum-Lithium-Copper Alloy : Influence of Electric Cycle, Electrolyte Bath Composition and Temperature**, *Surface Coating Technology*, 325, 627-635  
doi:https://doi.org/10.1016/j.surfcoat.2017.07.028
9. I. Mohammadi, A. Afshar, S. Ahmadi, ( 2016). **Al<sub>2</sub>O<sub>3</sub>/Si<sub>3</sub>N<sub>4</sub> Nanocomposite Coating On Aluminum Alloy by the Anodizing Route : Fabrication, Characterization, Mechanical Properties and Electrochemical Behavior**, *Ceram. Int* 42 12105-12114  
doi:https://doi.org/10.1016/j.ceramint.2016.04.142
10. P. H. Setyarini, R. Soenoko, Y. S. Irawan, Purnomo, (2018). **Corosion Characterization of Anodized AA 6061**. *MM Science Journal*, June  
doi:https://doi.org/10.17973/MMSJ.2018\_06\_201803  
doi:https://doi.org/0.1016/j.electacta.2010.02.044
11. T. Ito, Y. Matsuda, T. Jinba, N. Asai, T. Shimizu, Shingubara, S. (2017). **Fabrication and Characterization of Nano Porous Lattice Biosensor Using Anodic Aluminum Oxide Substrate**, *Japanese Journal of Applied Physics*, 56, 06GG02  
doi:https://doi.org/10.7567/JJAP.56.06GG02

12. O. O. Capraz, P. Shrotriya, P. Skeldon, G. E. Thompson, K. R. Hebert, (2015). **Role of Oxide Stress in the Initial Growth, of Self-Organized Porous Aluminum Oxide**, *Electrochimica Acta*, 167, 404-411  
doi: <https://doi.org/10.1016/j.electacta.2015.03.017>
13. J. Lee, D. Kim, C. H. Choi, W. Chung, (2017). **Nanoporous Anodic Alumina Oxide Layer and Its Sealing for the Enhancement of Radiative Heat Dissipation of Aluminum Alloy**, *Nano Energy*, 31, 504-513  
doi: <https://doi.org/10.1016/j.nanoen.2016.12.007>.
14. W. J. Stepniowski, M. Moneta, K. Karczewski, M. M. Domanska, T. Czujko, J. M. C. Mol, J. G. Buijnsters, (2018). **Fabrication of Copper, Nanowires Via Electrodeposition in Anodic Aluminum Oxide Templates Formed by Combined Hard Anodizing and Electrochemical Barrier Layer Thinning**, *Journal of Electroanalytic Chemistry*, 809, 59-66  
doi: <https://doi.org/10.1016/j.jelechem.2017.12.052>
15. F. A. Bruera, G. R. Kramer, M. L. Vera, A. E. Ares, (2019). **Synthesis and Morphological Characterization of Nanoporous Aluminum Oxide Films by Using A Single Anodizing Step**, *Coatings*, 9, 115  
doi: <https://doi.org/10.3390/coatings9020115>
16. H. Zhang, L. Yin, S. Shi, X. Liu, Y. Wang, F. Wang, (2015). **Facile and Fast Fabrication Method for Mechanically Robust Superhydrophobic Surface on Aluminum Foil**, *Microelectronic Engineering*, 141, 238-242  
doi: <https://doi.org/10.1016/j.mee.2015.03.048>
17. Y. Huang, D. Sarkar, X. Chen, (2016). **Fabrication of Corrosion Resistance Micro-Nanostructured Superhydrophobic Anodized Aluminum in One Step Electrodeposition Process**, *Metals*, 6, 47  
doi: <https://doi.org/10.3390/met6030047>.
18. Y. Qiu, S. Leung, Q. Zhang, C. Mu, B. Hua, H. Yan, S. Yang, Z. Fan, (2015) **Nanobowl optical concentrator for efficient light trapping and high-performance organic photovoltaics**. *Science Bulletin*, 60, 109-115.  
doi: <https://doi.org/10.1007/s11434-014-0693-8>.
19. S. F. Leung, M. Yu, Q. Lin, K. Kwon, K. L. Ching, L. Gu, K. Yu, Z. Fan, (2012). **Efficient photon capturing with ordered three-dimensional nanowell arrays**. *Nano Letters*, 2, 3682-3689.  
doi: <https://doi.org/10.1021/nl3014567>
20. Q. Lin, S. Leung, K. Tsui, B. Hua, Z. Fan, (2013). **Programmable nanoengineering templates for fabrication of three-dimensional nanophotonic structures**. *Nanoscale Research Letters*, 8, 268  
doi: <https://doi.org/10.1186/1556-276X-8-268>
21. Q. Lin, S. Leung, L. Lu, X. Chen, Z. Chen, H. Tang, W. Su, D. Li, Z. Fan, (2014). **Inverted nanocone-based thin film photovoltaics with omnidirectionally enhanced performance**. *ACS Nano*, 8, 6484-6490.  
doi: <https://doi.org/10.1021/nn5023878>.
22. Y. Gao, H. Jin, Q. Lin, X. Li, M. M. Tavakoli, S. Leung, W. M. Tang, L. Zhou, H. L. W. Chan, Z. Fan, (2015). **Highly flexible and transferable supercapacitors with ordered three-dimensional MnO<sub>2</sub>/Au/MnO<sub>2</sub> nanospikes arrays**. *Journal of Materials Chemistry A*, 3, 10199-10204. doi: <https://doi.org/10.1039/C5TA01960E>
23. S. Leung, L. Gu, Q. Zhang, K. Tsui, J. Shieh, C. Shen, T. Hsiao, C. Hsu, L. Lu, D. Li, Q. Lin, Z. Fan, (2014). **Roll-to-roll fabrication of large scale and regular arrays of three-dimensional nanospikes for high efficiency and flexible photovoltaics**. *Scientific Report*, 4, 4243. doi: <https://doi.org/10.1038/srep04243>
24. S. Leung, K. Tsui, Q. Lin, H. Huang, L. Lu, J. Shieh, C. Shen, C. Hsu, Q. Zhang, D. Li, (2014). **Large scale, flexible and three-dimensional quasi-ordered aluminum nanospikes for thin film photovoltaics with omnidirectional light trapping and optimized electrical design**. *Energy Environmental Science*, 7, 3611-3616.  
doi: <https://doi.org/10.1039/C4EE01850H>.
25. E. Julianto, W.A. Siswanto and M. Effendy (2019) **Characteristics of Temperature changes and Stress of Float Glass under Heat Radiation**, International Journal of Emerging Trends in Engineering Research 7(8), 228 – 233  
<https://doi.org/10.30534/ijeter/2019/03792019>
26. Majeed Ali Habeeb and Waleed Shaker Mahdi (2019) **Characterization of (CMC-PVP- Fe<sub>2</sub>O<sub>3</sub>) Nanocomposites for Gamma Shielding Application**, International Journal of Emerging Trends in Engineering Research 7(8), 247 – 255.  
<https://doi.org/10.30534/ijeter/2019/06792019>
27. Manish Bhandari (2020), **Numerical Solutions for Transverse Loading on Plate made of Functionally Graded Material**, International Journal of Emerging Trends in Engineering Research 7(8), 969 – 974.  
<https://doi.org/10.30534/ijeter/2020/05842020>